行政院國家科學委員會專題研究計畫 成果報告

形變影像對位法於PET/CT衰減矯正之應用
研究成果報告(精簡版)

計 畫 類 別 ：個別型
計 畫 編 號 ：NSC 99-2221-E-039-010-
執 行 期 間 ：99年08月01日至100年07月31日
執 行 單 位 ：中國醫藥大學生物醫學影像暨放射科學學系

計 畫 主 持 人 ：黃宗祺

報 告 附 件 ：出席國際會議研究心得報告及發表論文

處 理 方 式 ：本計畫可公開查詢

中 華 民 國 100年08月08日

Attenuation correction of PET images with interpolated average CT for thoracic tumors

2011 Phys. Med. Biol. 56 2559

(http://iopscience.iop.org/0031-9155/56/8/014)

IOP PUBLISHING PHYSICS IN MEDICINE AND BIOLOGY

Phys. Med. Biol. **56** (2011) 2559–2567 doi:10.1088/0031-9155/56/8/014

Attenuation correction of PET images with interpolated average CT for thoracic tumors

Tzung-Chi Huang[1,2], Greta S P Mok[3], Shyh-Jen Wang[1,4], Tung-Hsin Wu[1,6] and Geoffrey Zhang[5]

[1] Department of Biomedical Imaging and Radiological Sciences, National Yang Ming University, Taiwan
[2] Department of Biomedical Imaging and Radiological Science, China Medical University, Taiwan
[3] Department of Electrical and Electronics Engineering, Faculty of Science and Technology, University of Macau, Macau
[4] Department of Nuclear Medicine, Taipei Veterans General Hospital, Taiwan
[5] Department of Radiation Oncology, Moffitt Cancer Center, Florida, USA

E-mail: tung@ym.edu.tw

Received 26 November 2010, in final form 13 February 2011
Published 28 March 2011
Online at stacks.iop.org/PMB/56/2559

Abstract

To reduce positron emission tomography (PET) and computed tomography (CT) misalignments and standardized uptake value (SUV) errors, cine average CT (CACT) has been proposed to replace helical CT (HCT) for attenuation correction (AC). A new method using interpolated average CT (IACT) for AC is introduced to further reduce radiation dose with similar image quality. Six patients were recruited in this study. The end-inspiration and -expiration phases from cine CT were used as the two original phases. Deformable image registration was used to generate the interpolated phases. The IACT was calculated by averaging the original and interpolated phases. The PET images were then reconstructed with AC using CACT, HCT and IACT, respectively. Their misalignments were compared by visual assessment, mutual information, correlation coefficient and SUV. The doses from different CT maps were analyzed. The misalignments were reduced for CACT and IACT as compared to HCT. The maximum SUV difference between the use of IACT and CACT was ∼3%, and it was ∼20% between the use of HCT and CACT. The estimated dose for IACT was 0.38 mSv. The radiation dose using IACT could be reduced by 85% compared to the use of CACT. IACT is a good low-dose approximation of CACT for AC.

(Some figures in this article are in colour only in the electronic version)

[6] Author to whom any correspondence should be addressed.

Introduction

In modern positron emission tomography (PET) imaging, computed tomography (CT) has replaced Ge-68 for the transmission scan. The increased use of CT escalates the risk of radiation exposure for patients (Einstein *et al* 2007), and acquisition protocols need to be optimized according to the as low as reasonably achievable philosophy. The drawback of the helical CT (HCT) is the higher radiation dose as compared to Ge-68. Additionally, CT images are usually a snapshot of a respiration cycle, while PET scans are the results of the average of respiratory cycles. The temporal difference between the scans often introduces misalignment artifacts in PET images.

These misalignments especially introduce misleading tumor locations, volumes and standardized uptake values (SUVs) in diagnosing thoracic cancer and in radiation treatment planning (Beyer *et al* 2004, Charron *et al* 2000, Chin *et al* 2003, Kinahan *et al* 2003, Lardinois *et al* 2003, Schöder *et al* 2003, Schwaiger *et al* 2005, Townsend *et al* 2004, Zaidi and Hasegawa 2003). Reducing the mismatch between HCT and PET in PET/CT via the cine average CT (CACT) technique has been proposed (Cook *et al* 2007, Dawood *et al* 2009, Pan *et al* 2005). One concern is that its radiation dose is relatively high.

We previously described the use of the optical flow method (OFM), a deformable image registration algorithm, to register the CT pairs from different time phases and to provide a tissue motion map (Guerrero *et al* 2004, Zhang *et al* 2008). With this motion map, CT images representing the mid-phases of a respiratory cycle can be obtained by interpolation.

In this study, we develop and evaluate the feasibility of using interpolated average CT (IACT), generated from the end-expiration and -inspiration phases of cine CT and interpolated phases using deformable image registration, for the purpose of attenuation correction (AC). We also assess the potential dose reduction by using IACT.

Materials and methods

PET/CT data acquisition

Six cancer patients were recruited for this study. The tumor locations include left lower lobe, left anterior chest wall, right lower lobe, distal esophagus, right upper lobe, anterior mediastinum and right hilum. Images were acquired using a PET/CT scanner (Discovery VCT, GE Medical Systems, Milwaukee, WI, USA). All patients were injected with 298–458 MBq of ^{18}F-FDG and scanned 1 h after injection. The default acquisition settings of HCT data were as follows: 120 kV, smart mA (range 40–210 mA) (Kalra *et al* 2004), i.e. automatic tube current modulation to maintain constant image quality at the lowest dose for a different body anatomy, 1.375:1 pitch, 8 × 2.5 mm x-ray collimation, and 0.5 s CT gantry rotation. Cine CT data were acquired at 120 kV, 10 mA, 8 × 2.5 mm x-ray collimation, 0.5 s CT gantry rotation and 5.9 s cine CT duration which covers at least one breath cycle. A total of 13 phases in a respiratory cycle from the cine CT were averaged to generate the CACT (Pan *et al* 2005). PET data were acquired at the 3 min per 15 cm bed position. Our protocol was approved by the local ethics committee and the subject number was kept to be minimal, while still showing the significance of the proposed method, to avoid unnecessary radiation exposure. Written informed consents were obtained from all patients.

Deformable image registration

The OFM (Guerrero *et al* 2004, Zhang *et al* 2008) was applied to calculate the velocity matrix on two successive CT images in cine CT. The velocity matrix includes lateral,

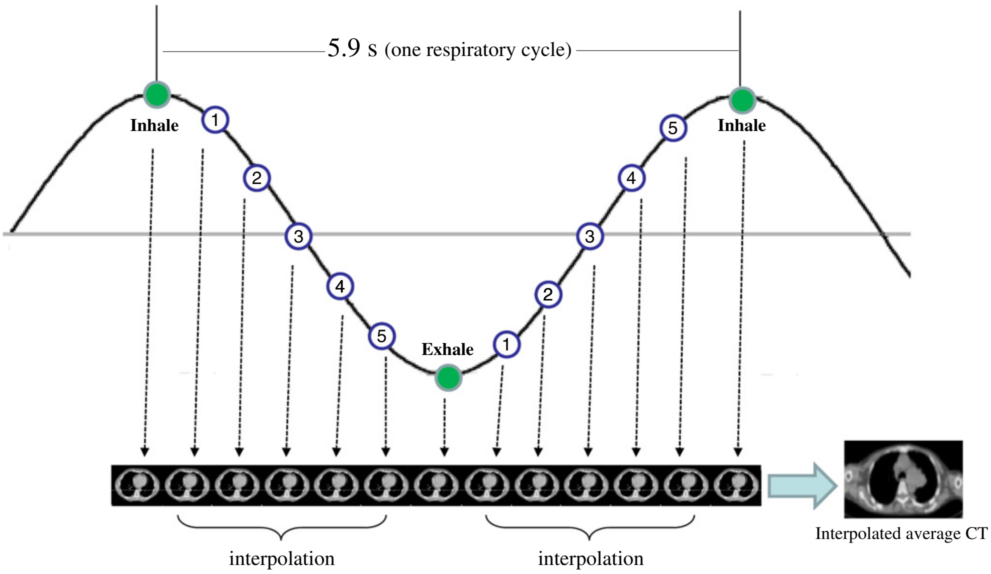

Figure 1. The generation of IACT. The two extreme phases in cine CT, end-inspiration and -expiration, are registered using the OFM. The resultant deformation matrix is then used to interpolate the phases in between with equal temporal intervals. $\mathrm{IACT}_{2\mathrm{o}11\mathrm{i}}$, used for AC in PET reconstruction, is the average of the 2 original phases and the interpolated 11 phases.

anterior–posterior and inferior–superior displacements for each voxel, respectively. The OFM calculation equation is as follows:

$$v^{(n+1)} = v^{(n)} + \nabla f \left(\frac{\nabla f \cdot v^{(n)} + \frac{\partial f}{\partial t}}{\alpha^2 + \|\nabla f\|^2} \right), \tag{1}$$

where n is the number of iterations, $v^{(n)}$ is the average velocity driven from the surrounding voxels, f is the image intensity, and α is the weighting factor whose value is empirically set at 5 for the OFM in CT (Huang *et al* 2010, Zhang *et al* 2008).

Interpolated average CT

For IACT calculated from 2 original phases + 11 interpolated phases ($\mathrm{IACT}_{2\mathrm{o}11\mathrm{i}}$), two extreme phases in cine CT, i.e. normal end-inspiration and -expiration, are used to generate the motion maps via the OFM. The total motion range for each voxel in the forward motion map is equally spaced into six intervals, resulting in five sets of interpolated CT images as the mid-phases from inspiration to expiration. Similarly, the backward motion map is used to calculate the five mid-phases from expiration to inspiration (figure 1). The ten interpolated phases together with the two original phases, plus the next inhalation compose a complete respiratory cycle. These 13 phases are averaged to generate the $\mathrm{IACT}_{2\mathrm{o}11\mathrm{i}}$.

To study the reliability of the proposed IACT technique, different numbers of original phases in the cine CT are used in calculating IACT. Other configurations of the IACTs include 4 original phases + 9 interpolated phases ($\mathrm{IACT}_{4\mathrm{o}9\mathrm{i}}$), 6 original phases + 7 interpolated phases ($\mathrm{IACT}_{6\mathrm{o}7\mathrm{i}}$), and 8 original phases + 5 interpolated phases ($\mathrm{IACT}_{8\mathrm{o}5\mathrm{i}}$).

Image reconstruction

All PET images were reconstructed using the OS-EM reconstruction method with 2 iterations and 28 subsets. AC were conducted using the obtained CT maps: HCT, CACT, IACT (IACT_{2o11i}, IACT_{4o9i}, IACT_{6o7i}, IACT_{8o5i}), and average CT was obtained from two extreme phases (ACT). Their reconstructed PET images were compared and their differences in image quality and associated radiation dose were quantified.

Data analysis

Mutual information. In order to provide the overlap invariance, normalized mutual information (MI) was utilized (Studholme *et al* 1999). The normalized MI between X and Y, denoted as $I(X, Y)$, is a measure of the statistical dependence between both variables, defined as in equation (2). In this study, normalized MI was applied to estimate the nonlinear image intensity distribution between IACT/HCT/ACT and CACT:

$$I(X, Y) = \frac{P(X) + P(Y)}{P(X, Y)}, \tag{2}$$

where $P(X)$ is the histogram of X, $P(Y)$ is the histogram of Y and $P(X, Y)$ is the joint histogram of X and Y. MI represents how much the knowledge of X decreases the uncertainty of Y. Therefore, $I(X, Y)$ is a measure of the shared information between X and Y. The larger the normalized MI values, the more similar two images are (Studholme *et al* 1999, Zhang *et al* 2008).

Correlation coefficient. The correlation coefficient (CC) was applied to calculate the linear intensity relationship point by point between IACT/HCT/ACT and CACT. The CC value represents the total intensity difference between two image sets, i.e. the summation of the intensity difference for all n voxels. The equation defining the CC is

$$\mathrm{CC} = \frac{S_{u,v}}{S_u \times S_v} = \frac{\sum_{i=1}^{n} (u_i - \overline{u}) \times (v_i - \overline{v})}{\sqrt{\sum_{i=1}^{n} (u_i - \overline{u})^2} \times \sqrt{\sum_{i=1}^{n} (v_i - \overline{v})^2}} \tag{3}$$

where S_u is the standard deviation of object u, S_v is the standard deviation of object v, and $S_{u,v}$ is the covariance of objects u and v. The value of the CC is between -1 and 1, indicating negatively correlated to positively correlated, respectively.

Both MI and CC methods are capable of giving a quantitative measure of similarity between CT images. Since they have different sensitivities to different components of differences, both are included in this study to demonstrate their usage in similarity comparison.

Standardized uptake value. The PET images reconstructed using HCT, CACT and IACT for AC were compared by visual assessment. The same volumes-of-interest (VOIs) were delineated at the same location around the tumor and the average SUVs in the VOI were obtained. The average SUVs were compared using the following equation:

$$\mathrm{diff}_{\mathrm{IACT-CACT}} = \frac{|\mathrm{SUV}_{\mathrm{IACT}} - \mathrm{SUV}_{\mathrm{CACT}}|}{\mathrm{SUV}_{\mathrm{CACT}}} \times 100\%. \tag{4}$$

The differences between the HCT/ACT and CACT techniques, $\mathrm{diff}_{\mathrm{HCT-CACT}}$ and $\mathrm{diff}_{\mathrm{ACT-CACT}}$, were also calculated by replacing IACT with HCT/ACT in the above equation. Smaller values of $\mathrm{diff}_{\mathrm{IACT-CACT}}$, $\mathrm{diff}_{\mathrm{HCT-CACT}}$ and $\mathrm{diff}_{\mathrm{ACT-CACT}}$ indicate better estimations of the CACT technique, i.e. less misalignment errors between the associated CT and PET images.

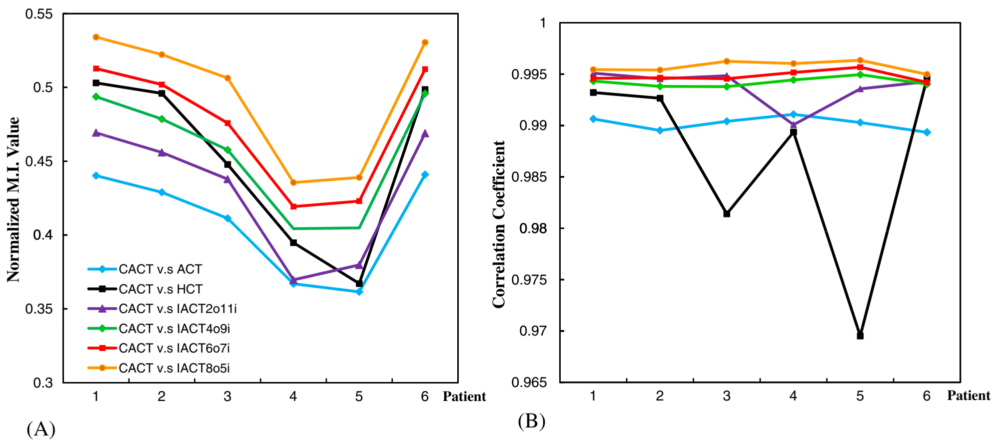

Figure 2. (A) Values of normalized MI between HCT, ACT, CACT and IACT with different configurations. (B) Values of CC between HCT, ACT, CACT and IACT with different configurations.

Radiation dose

Radiation dose was expressed using the volume CT dose index ($\mathrm{CTDI_{vol}}$) in Gy, and effective dose in mSv. The dose–length product is defined as the $\mathrm{CTDI_{vol}}$ multiplied by the scan length, and is an indicator of the integrated radiation dose of an entire CT examination. An approximation of the effective dose was obtained by multiplying the dose–length product by a conversion factor, k (equal to 0.017 mSv $\mathrm{mGy^{-1}\ cm^{-1}}$) (ICRP 2007).

Results

The MI and CC results showed that as the number of original phases in IACT increases, IACT and CACT become more relevant, while $\mathrm{IACT_{2o11i}}$ performs better than ACT (figure 2). Figure 3 shows the sample reconstructed images of HCT, CACT and $\mathrm{IACT_{2o11i}}$, their associated PET images and the fused PET/CT images. The only noticeable difference between CACT and $\mathrm{IACT_{2o11i}}$ is the higher noise level in $\mathrm{IACT_{2o11i}}$ as compared to CACT. This is expected as CACT is an average of all 13 original phases from cine CT, while $\mathrm{IACT_{2o11i}}$ uses only 2 original phases. On the other hand, PET images using HCT for AC demonstrate noticeable artifacts in the diaphragm region. The SUV analysis for HCT, CACT, different IACTs and ACT is shown in figure 4. For tumor nos 1 through 7, the difference from the one using CACT is smallest when $\mathrm{IACT_{8o5i}}$ is used, and it is largest when HCT is used. However, even with $\mathrm{IACT_{2o11i}}$ where the difference is the largest among all IACT configurations, it is $\leqslant 3\%$ as compared to CACT, while the difference was $\geqslant 10\%$ with the maximum difference of $\sim 20\%$, between the use of HCT and CACT, consistent with the reported values (Pan *et al* 2005). The results of ACT are generally inferior to those of $\mathrm{IACT_{2o11i}}$ except for tumor no 4.

The effective radiation doses (and $\mathrm{CTDI_{vol}}$) from the CT scans are listed in table 1. The higher dose from HCT, 5.28 mSv (11.18 mGy), is due to the clinical setting of smart mA. In cine CT, the current is set at 10 mA; thus the effective dose is 2.46 mSv (5.17 mGy). If the two original phases in the $\mathrm{IACT_{2o11i}}$ are replaced by two breath-hold CT scans with the same tube current as of cine CT, the effective dose would be 0.38 mSv (0.79 mGy), i.e. an 85% reduction from cine CT and a 93% reduction from HCT. In addition, the typical effective

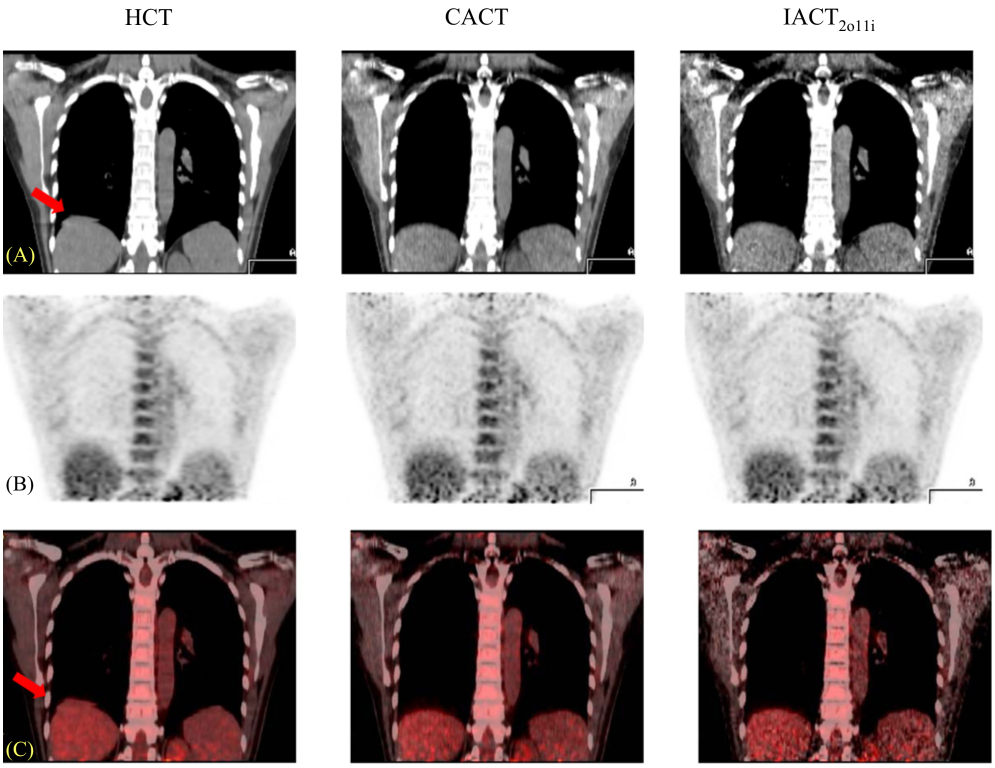

Figure 3. (A) Sample reconstructed images of HCT, CACT and $IACT_{2o11i}$, (B) their associated attenuation-corrected PET images and (C) PET/CT fused images. Noticeable misalignment artifacts in the diaphragm region (arrow) can be found in the HCT-corrected PET.

Table 1. HCT, CACT and IACT scanning parameters and doses estimation.

	HCT	CACT	$IACT_{2\text{-breath-hold CT}}$
Scan mode	Helical mode	Axial cine mode	Helical mode
Tube voltage (kVp)	120	120	120
Tube current (mA)	40–210	10	10
Number of phases	1	13	2
$CTDI_{vol}$ (mGy)	11.18	5.17	0.79
Scan coverage (cm)	28	28	28
Dose–length product (mGy cm)	310.49	144.62	22.25
Effective dose (mSv)	5.28	2.46	0.38

dose from ^{18}F-FDG PET imaging is about 10.73 mSv which is invariant with the AC method (Deloar *et al* 1998, Wu *et al* 2005).

Discussion

The OFM establishes the link between two extreme respiratory phases. With the interpolated phases added, the whole respiratory cycle is constructed. Our results showed that $IACT_{2o11i}$

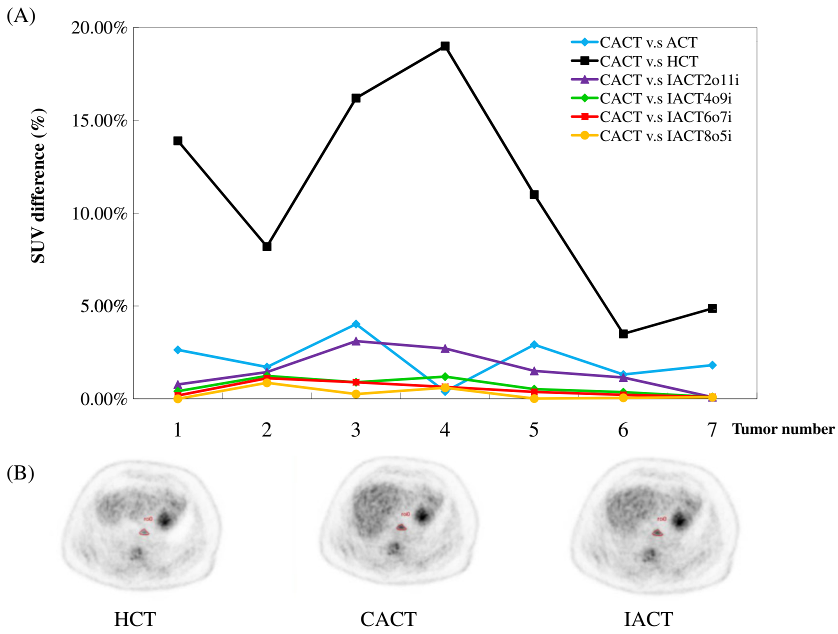

Figure 4. (A) SUV difference between PET images corrected by HCT, ACT, CACT and IACT with different configurations. (B) Transaxial PET images at the lesion level corrected by (left) HCT images, (middle) CACT images and (right) $IACT_{2o11i}$ images.

generally outperforms ACT, demonstrating the effectiveness of this method. The little difference in the SUV for PET using IACT and CACT for AC also indicates that IACT is a good approximation of CACT, with the advantage of less radiation dose. For gated PET studies, other approaches for AC are proposed. For example, respiratory gated CT corresponding to the gated PET frames are acquired for phase-dependent AC. Other methods include transforming a single CT image to match the associated PET frames through tracking the diaphragm motions in PET (McQuaid *et al* 2009). These methods require manual segmentation of the diaphragm and their accuracy highly depends on the motion model.

The motion amplitude may impact the accuracy of the motion maps. Zhong *et al* (2010) showed that the average error in deformable image registration in thoracic regions was around 0.7 mm for a diaphragm motion of 2.6 cm. This accuracy is sufficient for PET AC as PET resolution is much coarser.

The selected lesions located in diversified thoracic regions are representative of general clinical scenarios. Chi *et al* (2008) reported that out of 216 lung cancer patients, 68% had mis-registration and only 10% had an SUV change of >25% at the tumor location. Four out of seven lesions in our study showed >10% SUV difference between the use of CACT and HCT, with the maximum SUV difference of ∼20% for the esophageal lesion which is closest to the diaphragm among all cases.

The drawback of the very low dose setting (10 mA) in both CACT and IACT methods is the increased noise in the CT images. Noisy AC data can introduce noise into the PET emission images. As shown in figure 3(B), the emission data for CACT and IACT appear noisier than the images corrected with HCT data because of the higher quantum noise in the AC data in CACT and IACT. If the same signal-to-noise ratio in the emission images of the HCT method is desired, the current setting in CACT and IACT has to be the same as that in the HCT method. The dose to the patient would be higher for the IACT method as compared with HCT, but still much lower than that in CACT. As the purpose of the PET images is to obtain accurate SUV and tumor location and shape, as long as the noise in PET does not affect the extraction of such information, the very low dose setting should be sufficient for a reasonable AC CT quality.

It should be noted that the proposed method may not produce better PET image quality as compared with CACT either. The quality of each phase CT in a low-dose 4DCT set is sufficient for clinicians to read. The very low dose breath-hold CT should possess at least the same quality of each phase of the CT in the 4DCT as the current and voltage settings are the same, with the residual motion, which often exists in each phase of 4DCT, not present in the breath-hold CT. The major advantage of the proposed IACT method is less dose to the patient and yet a good approximation of the CACT method in the SUV and tumor location.

Clinically, two extreme phases in cine CT can be replaced by two separate CT scans, one at normal end-inspiration and the other at end-expiration. Since breath-hold CTs are likely different from the phases in free-breathing cine CT, an active breath control (ABC) system, originally developed by Wong *et al* (1999) for clinical radiotherapy, can be used to ensure breath-hold CTs being taken at desired phases. This non-invasive device integrates a spirometer with a personal computer to control the flow meters and scissor valves. A nose clip is used to ensure that the patients only breathe via the mouthpiece. Patients can be trained using this device prior to the actual CT scanning, and CT images can then be taken at desirable lung volume, i.e. a particular phase of the breathing cycle. Partridge *et al* (2009 showed that a breath-holding time of 15–30 s can be achieved for patients with lung cancer. Further study with real breath-hold CT data using ABC is warranted.

Conclusion

The application of IACT for PET AC reduces misalignment artifacts and SUV quantification errors for thoracic tumors as compared to that of HCT. The radiation dose using IACT could be reduced by 85% compared to that of CACT. It serves as a low-dose alternative to CACT. Further study with separate CT scans placed at end-expiration and -inspiration phases is needed.

Acknowledgments

We would like to thank Mr Martin J Stumpf of the Division of Medical Imaging at Johns Hopkins University for proofreading and editing the manuscript. This study was financially supported in part by the National Science Council of Taiwan (NSC 99-2221-E-039-010) and by the school project of China Medical University, Taiwan (CMU98-C-10). The project was conducted in the campus of NYMU/TVGH.

References

Beyer T, Antoch G, Muller S, Egelhof T, Freudenberg L S, Debatin J and Bockisch A 2004 Acquisition protocol considerations for combined PET/CT imaging *J. Nucl. Med.* **45** 25S–35S

Charron M, Beyer T, Bohnen N N, Kinahan P E, Dachille M, Jerin J, Nutt R, Meltzer C C, Villemagne V and Townsend D W 2000 Image analysis in patients with cancer studied with a combined PET and CT scanner *Clin. Nucl. Med.* **25** 905–10

Chi P-C M, Mawlawi O, Luo D, Liao Z, Macapinlac H A and Pan T 2008 Effects of respiration-averaged computed tomography on positron emission tomography/computed tomography quantification and its potential impact on gross tumor volume delineation *Int. J. Radiat. Oncol. Biol. Phys.* **71** 890–9

Chin B B, Nakamoto Y, Kraitchman D L, Marshall L and Wahl R 2003 PET-CT evaluation of 2-deoxy-2-[18F] fluoro-D-glucose myocardial uptake: effect of respiratory motion *Mol. Imag. Biol.* **5** 57–64
Cook R A H, Carnes G, Lee T-Y and Wells R G 2007 Respiration-averaged CT for attenuation correction in canine cardiac PET/CT *J. Nucl. Med.* **48** 811–8
Dawood M, Büther F, Stegger L, Jiang X, Schober O, Schäfers M and Schäfers K P 2009 Optimal number of respiratory gates in positron emission tomography: a cardiac patient study *Med. Phys.* **36** 1775–84
Deloar H M, Fujiwara T, Shidahara M, Nakamura T, Watabe H, Narita Y, Itoh M, Miyake M and Watanuki S 1998 Estimation of absorbed dose for 2-[F-18]fluoro-2-deoxy-glucose using whole-body positron emission tomography and magnetic resonance imaging *Eur. J. Nucl. Med. Mol. Imag.* **25** 565–74
Einstein A J, Moser K W, Thompson R C, Cerqueira M D and Henzlova M J 2007 Radiation dose to patients from cardiac diagnostic imaging *Circulation* **116** 1290–305
Guerrero T, Zhang G, Huang T-C and Lin K-P 2004 Intrathoracic tumour motion estimation from CT imaging using the 3D optical flow method *Phys. Med. Biol.* **49** 4147–61
Huang T-C, Liang J-A, Dilling T, Wu T-H and Zhang G 2010 Four-dimensional dosimetry validation and study in lung radiotherapy using deformable image registration and Monte Carlo techniques *Radiat. Oncol.* **5** 45
ICRP 2007 Managing patient dose in multi-detector computed tomography (MDCT): ICRP Publication 102 *Ann. ICRP* **37** 1–80
Kalra M K, Maher M M, Toth T L, Schmidt B, Westerman B L, Morgan H T and Saini S 2004 Techniques and applications of automatic tube current modulation for CT *Radiology* **233** 649–57
Kinahan P E, Hasegawa B H and Beyer T 2003 X-ray-based attenuation correction for positron emission tomography/computed tomography scanners *Semin. Nucl. Med.* **33** 166–79
Lardinois D, Weder W, Hany T F, Kamel E M, Korom S, Seifert B, von Schulthess G K and Steinert H C 2003 Staging of non-small-cell lung cancer with integrated positron-emission tomography and computed tomography *N. Engl. J. Med.* **348** 2500–7
McQuaid S J, Lambrou T, Cunningham V J, Bettinardi V, Gilardi M C and Hutton B F 2009 The application of a statistical shape model to diaphragm tracking in respiratory-gated cardiac PET images *Proc. IEEE* **97** 2039–52
Pan T, Mawlawi O, Nehmeh S A, Erdi Y E, Luo D, Liu H H, Castillo R, Mohan R, Liao Z and Macapinlac H A 2005 Attenuation correction of PET images with respiration-averaged CT images in PET/CT *J. Nucl. Med.* **46** 1481–7
Partridge M, Tree A, Brock J, McNair H, Fernandez E, Panakis N and Brada M 2009 Improvement in tumor control probability with active breathing control and dose escalation: a modeling study *Radiother. Oncol.* **91** 325–9
Schöder H, Erdi Y, Larson S and Yeung H D 2003 PET/CT: a new imaging technology in nuclear medicine *Eur. J. Nucl. Med. Mol. Imag.* **30** 1419–37
Schwaiger M, Ziegler S and Nekolla S G 2005 PET/CT: challenge for nuclear cardiology *J. Nucl. Med.* **46** 1664–78
Studholme C, Hill D L G and Hawkes D J 1999 An overlap invariant entropy measure of 3D medical image alignment *Pattern Recognit.* **32** 71–86
Townsend D W, Carney J P J, Yap J T and Hall N C 2004 PET/CT today and tomorrow *J. Nucl. Med.* **45** 4S–14S
Wong J W, Sharpe M B, Jaffray D A, Kini V R, Robertson J M, Stromberg J S and Martinez A A 1999 The use of active breathing control (ABC) to reduce margin for breathing motion *Int. J. Radiat. Oncol. Biol. Phys.* **44** 911–9
Wu T-H, Chu T-C, Huang Y-H, Chen L-K, Mok S-P, Lee J-K, Yeu-Sheng T and Lee J J S 2005 A positron emission tomography/computed tomography (PET/CT) acquisition protocol for CT radiation dose optimization *Nucl. Med. Commun.* **26** 323–30
Zaidi H and Hasegawa B 2003 Determination of the attenuation map in emission tomography *J. Nucl. Med.* **44** 291–315
Zhang G, Huang T-C, Guerrero T, Lin K-P, Stevens C, Starkschall G and Forster K 2008 Use of three-dimensional (3D) optical flow method in mapping 3D anatomic structure and tumor contours across four-dimensional computed tomography data *J. Appl. Clin. Med. Phys.* **9** 59–69
Zhong H, Kim J and Chetty I J 2010 Analysis of deformable image registration accuracy using computational modeling *Med. Phys.* **37** 970–9

教師出席國際學術會議報告

98 年 7 月 17 日

報告人姓名	黃宗祺	服務單位及職稱	放射技術學系
時間 會議 地點	自 100 年 7 月 3 日至 100 年 7 月 7 日，Zurich 蘇黎世, Swiss 瑞士		
會議 名稱	（中文）第 13 屆放射影像偵測器國際研討會 （英文）13th International Workshop on Radiation Imaging Detectors		
發表 論文 題目	Poster （中文）使用劑量膠進行三維輻射劑量驗證 （英文）Three-dimensional dose verification using normoxic polymer gel dosimeters for tomotherpay		

報告內容應包括下列各項：

一、參加會議經過

張貼海報並與國際學者互相討論各自研究心得，會中聆聽國際學者的口頭報告。於會議餐會，結識外國學者，邀請國外學者有機會至我們學校演講並分享相關研究心得。，

二、與會心得

影像處理技術在放射科學應用為目前非常熱門的題目，在目前幾個大型研討會，皆有專門的 SECTION，參與發表與討論者很多，應用技術減少病人對放射性的吸收，減低併發症機率提升醫療治癒率，是全世界上醫事放射人員的目標。

三、考察參觀活動(無是項活動者省略)

四、建議

放射照影與治療技術一日千里，每隔一段時間就有新技術與儀器出來，新的技術與儀器對病人都有實質上的幫助，希望學校或附設醫院，能多補助老師與醫事人員進修或參與研討會，以期增進學校與附設醫院的競爭力。

五、攜回資料名稱及內容

1. 參與海報（附件一）
2. 研討會論文集

六、其他

附件一

Three-dimensional Dose Verification Using Normoxic Polymer Gel Dosimeters for Tomotherapy

Tung-Hsin Wu[1], Chien-Yi Hsiao[2], Mu-Bai Chang[2], Geoffrey Zhang[3], Ji-An Lian[2] and Tzung-Chi Huang[2*]

[1]Department of Biomedical Imaging and Radiological Sciences, National Yang Ming University, Taiwan, R.O.C
[2]Department of Biomedical Imaging and Radiological Science, China Medical University, Taiwan, R.O.C
[3]Department of Radiation Oncology, Moffitt Cancer Center, Florida, USA

ABSTRACT

The aim of this study is to evaluate the feasibility of using MAGAT as a near real-time 3-dimensional dose measurement device for tomotherapy. MAGAT is a new type of normoxic polymer gel dosimeter, which responses well to absorbed dose and can be easily made in the presence of normal oxygen surroundings. Its dose response was measured by irradiating MAGAT-gel-filled testing vials with tomotherapy and its linear relationship with dose was present from 0 to 6.6 Gy. One group of gel samples were measured in near real-time, in which the gel phantom was read right after the irradiation. The other group was measured 12 hours after irradiation so the gel phantom can be exposed to oxygen. Several post-imaging processing filters including Nagao, Guess, median, mean, min and max, were applied on megavoltage computed tomography (MVCT) images for better discimination on dose responses. Our results show that dose responses for MVCT with real-time and 12-hour delayed measurement were 4.76 and 4.69 ΔSI · cGy⁻¹, respectively, and show no significant difference (p-value = 0.72). For study of the filtering effects, Gauss, median and mean filters offer better linear correction coefficients of dose response. In conclusion, the MAGAT polymer gel dosimeter read from MVCT imaging is a promising method for dose verification in clinical tomotherapy.

CONTACT

INTRODUCTION

Tomotherapy delivers radiation using a rotating intensity-modulated fan beam geometry, and the modulation varies with gantry angle. Because the resultant dose-distributions comprise modulated contributions from many angles, the system has the potential to deliver highly conformal treatments. It was designed to be a purpose-built image guided radiotherapy (IGRT) machine. The capability for continuous rotation, coupled with translation of the patient through the gantry, allows helical treatment arcs in a way similar to helical or spiral diagnostic CT scanners. The helical tomotherapy accelerator is mounted on a slip ring gantry. This allowed a CT detector array (Xenon filled linear array) to be mounted opposite the source. The primary purpose of this detector is for megavoltage computed tomography (MVCT), delivery verification, and dose reconstruction [1,2]. This on-board linear array of ion chambers also has demonstrated its advantage for quality assurance and beam alignment commissioning [3]. Additionally, it has also proved useful for quantifying required dose planning parameters.

METHODS AND MATERIALS

The clinical helical tomotherapy unit (TomoTherapy Inc., Madison, Wisconsin, USA) consists of a 6-MV linear accelerator with a binary multi-leaf collimator and a xenon CT detector system. The MVCT mode of the linear accelerator reduces the nominal energy to about 3.5 MV, and transverse 4-mm MVCT images were obtained. This results in the acquisition of volumetric images at acceptable doses, typically between 0.5 cGy and 3 cGy, which are comparable with doses required from planar images on contemporary MV electronic portal imaging devices (EPIDs).

The MAGAT normoxic polymer gel was prepared under normal oxygen conditions using gelatin, methacrylic acid, THPC solution, as an oxygen scavenger, and distilled water (high performance liquid chromatography grade). The gelatin was given to distilled water and heated to 50 C in a water bath. A clear solution was achieved and cooled down to 35 C. The methacrylic acid and THPC solution were then added to the gelatin solution. A homogeneous liquid mixture was achieved by continuous stirring. All gels were prepared and poured into 50 ml plastic vials of 25 mm in diameter and 115 mm in height and filled to the top to minimize oxygen presence in the vials. A study has indicated that gels need to be exposed to oxygen for at least 12 hr after irradiation to terminate their intrinsic polymerization reactions and then MVCT can be used as a reading device .

RESULTS & Discussion

MAGAT gel dosimeter has the advantages of 3D dose measurement, tissue equivalence, high dose sensitivity, easy preparation, low cost, capability of accumulative dose measurement and its signal is not spreading with time. However, one needs to be cautious in temperature and composition control in preparation to avoid hydrolysis and polymerization. Incomplete prepared gel dosimeter also affects the dose response. The dose delivered by the MVCT to the dosimeter is about 1% of a fractional dose in radiotherapy treatment. The additional dose from the MVCT scan is thus within the tolerance. The higher the dose absorbed by the dosimeter, the higher the attenuation to the MVCT photons by the gel. The response is linear to the absorbed dose within the dose range in radiotherapy.

The tomotherapy unit is the dose delivering system and its MVCT is the dose reading system when MAGAT polymer dosimeter is used, which not only provides a robust treatment quality assurance system, but also warrants the measurement consistency.

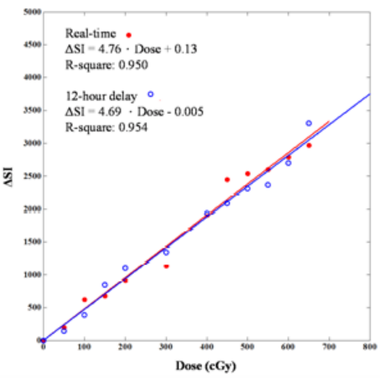

Figure 1. Figure 1. Dose response curves of real-time reading (●) and 12 hours delay reading ( ). The horizontal axis is the absorbed dose in cGy, and the vertical axis is the MVCT signal intensity difference, ΔSI.

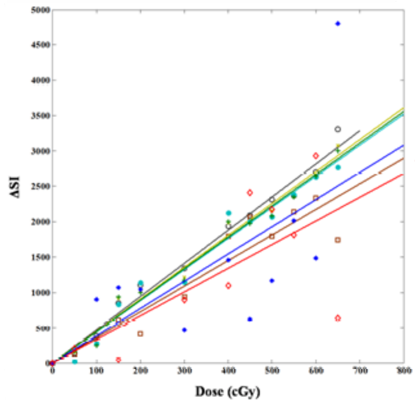

Figure 2. Dose response curves for 12 hours delayed reading with no filter( ) and with Nagao ( ), Gauss (x), median (●), mean (+), max (∗) and min ( ) filters. The horizontal axis is the absorbed dose in cGy, and the vertical axis is the MVCT signal intensity difference, ΔSI.

CONCLUSIONS

In this work, we have investigated the dose response curves for MAGAT polymer gel dosimeter using tomotherapy as the dose delivering machine and its MVCT as the 3D dose reader. This study is the first attempt to explore the potential role of using MVCT as a reading device for gel dosimeters. The dose responses, measured at different MVCT imaging times, showed no significantly difference. For effects of different filters, Gauss, median and mean filters offer better linear correction coefficients of dose response. In conclusion, normoxic polymer gel dosimeter combined with MVCT as a dose reading device provides a useful method for tomotherapy in three-dimensional real-time dose measurement and verification.

ACKNOWLEDGEMENTS

■ This study was financially supported by the National Science Council of Taiwan. NSC 98-2221-E-039-010

表 Y04

國科會補助計畫衍生研發成果推廣資料表

日期:2011/08/08

國科會補助計畫	計畫名稱: 形變影像對位法於PET/CT衰減矯正之應用
	計畫主持人: 黃宗祺
	計畫編號: 99-2221-E-039-010- 學門領域: 醫學資訊

無研發成果推廣資料

99 年度專題研究計畫研究成果彙整表

計畫主持人：黃宗祺　　**計畫編號：**99-2221-E-039-010-

計畫名稱：形變影像對位法於 PET/CT 衰減矯正之應用

成果項目			量化：實際已達成數（被接受或已發表）	量化：預期總達成數(含實際已達成數)	量化：本計畫實際貢獻百分比	單位	備註（質化說明：如數個計畫共同成果、成果列為該期刊之封面故事...等）
國內	論文著作	期刊論文	0	0	100%	篇	
		研究報告/技術報告	0	0	100%		
		研討會論文	0	0	100%		
		專書	0	0	100%		
	專利	申請中件數	0	0	100%	件	
		已獲得件數	0	0	100%		
	技術移轉	件數	0	0	100%	件	
		權利金	0	0	100%	千元	
	參與計畫人力（本國籍）	碩士生	1	1	100%	人次	
		博士生	1	1	100%		
		博士後研究員	0	0	100%		
		專任助理	0	0	100%		
國外	論文著作	期刊論文	1	1	100%	篇	
		研究報告/技術報告	0	0	100%		
		研討會論文	0	0	100%		
		專書	0	0	100%	章/本	
	專利	申請中件數	0	0	100%	件	
		已獲得件數	0	0	100%		
	技術移轉	件數	0	0	100%	件	
		權利金	0	0	100%	千元	
	參與計畫人力（外國籍）	碩士生	0	0	100%	人次	
		博士生	0	0	100%		
		博士後研究員	0	0	100%		
		專任助理	0	0	100%		

其他成果 (無法以量化表達之成果如辦理學術活動、獲得獎項、重要國際合作、研究成果國際影響力及其他協助產業技術發展之具體效益事項等，請以文字敘述填列。)	無

	成果項目	量化	名稱或內容性質簡述
科教處計畫加填項目	測驗工具(含質性與量性)	0	
	課程/模組	0	
	電腦及網路系統或工具	0	
	教材	0	
	舉辦之活動/競賽	0	
	研討會/工作坊	0	
	電子報、網站	0	
	計畫成果推廣之參與（閱聽）人數	0	

國科會補助專題研究計畫成果報告自評表

請就研究內容與原計畫相符程度、達成預期目標情況、研究成果之學術或應用價值（簡要敘述成果所代表之意義、價值、影響或進一步發展之可能性）、是否適合在學術期刊發表或申請專利、主要發現或其他有關價值等，作一綜合評估。

1. 請就研究內容與原計畫相符程度、達成預期目標情況作一綜合評估 ■達成目標 □未達成目標（請說明，以 100 字為限） 　　□實驗失敗 　　□因故實驗中斷 　　□其他原因 說明：
2. 研究成果在學術期刊發表或申請專利等情形： 論文：■已發表 □未發表之文稿 □撰寫中 □無 專利：□已獲得 □申請中 ■無 技轉：□已技轉 □洽談中 ■無 其他：（以 100 字為限）
3. 請依學術成就、技術創新、社會影響等方面，評估研究成果之學術或應用價值（簡要敘述成果所代表之意義、價值、影響或進一步發展之可能性）（以 500 字為限） 1. 突破初期影像處理演算法的瓶頸，增進影像對位技術在臨床醫學影像的適用性。 2. 發表研究成果，並完成學術論文之投稿，貢獻並提昇國內學術水準。 3. 本計畫進行之人員包含學校研究人員、臨床核醫科醫師、臨床醫學放射師，跨越學術與臨床，在團對工作中交換研究心得，在學術與臨床互相結合，達到產學合作之目的。